Paleobiology, 32(2), 2006, pp. 278–298

Modeling shelliness and alteration in shell beds: variation in hardpart input and burial rates leads to opposing predictions

Adam Tomašových, Franz T. Fürsich, and Thomas D. Olszewski

Abstract.—Distinguishing the differential roles of *hardpart-input rates* and *burial rates* in the formation of shell beds is important in paleobiologic and sedimentologic studies, because high shelliness can reflect either high population density of shell producers or lack of sediment. The modeling in this paper shows that differences in the relative importance of burial rates and hardpart-input rates lead to distinct patterns with respect to the degree of shelliness and taphonomic alteration in shell beds. Our approach substantially complements other models because it allows computation of both shelliness and assemblage-level alteration. To estimate shelliness, we dissected hardpart-input rates into dead-shell production and shell destruction rates. To estimate assemblage-level alteration, we computed an alteration rate that describes how rapidly shells accrue postmortem damage. Under decreasing burial rates but constant hardpart-input rates, a *positive* correlation between alteration and shelliness is expected (Kidwell's R-sediment model). In contrast, under decreased destruction rates and/or increased dead-shell production rates and constant burial rates (Kidwell's R-hardpart model), a *negative* correlation between shelliness and alteration is expected. The contrasting predictions thus provide a theoretical basis for distinguishing whether high shell density in shell beds reflects passive shell accumulation due to a lack of sediment dilution or whether it instead reflects high shell input from a life assemblage. This approach should be applicable for any fossil assemblages that vary in shell density and assemblage-level alteration. An example from the Lower Jurassic of Morocco, which has shell-rich samples less altered than shell-poor samples, suggests that the higher shelliness correlates with higher community-level abundance and lower proportion of juveniles of the main shell producer, supporting the driving role of hardpart-input rates in the origin of the shell-rich samples in this case. This is of significance in paleoecologic analyses because variations in shelliness can directly reflect fluctuations in population density of shell producers.

Adam Tomašových and Franz T. Fürsich. Institut für Paläontologie, Würzburg Universität, Pleicherwall 1, 97070 Würzburg, Germany. E-mail: adam.tomasovych@mail.uni-wuerzburg.de, E-mail: franz.fuersich@mail.uni-wuerzburg.de*

Thomas D. Olszewski. Department of Geology and Geophysics and Faculty of Ecology and Evolutionary Biology, Texas A&M University, College Station, Texas 77843. E-mail: tomo@geo.tamu.edu

* Present address*: Geological Institute of Slovak Academy of Sciences, Dúbravska cesta 9, 84005 Bratislava, Slovakia*

Accepted: 11 October 2005

Introduction

Recognizing the differential role of sedimentation rates and hardpart-input rates (i.e., dead-shell production and shell destruction rates) in shell bed formation is important because high shell density in death assemblages can result from lack of sediment or high input of shells from a life assemblage. One of the main taphonomic paradigms in interpreting marine shell beds is that sites of slow net rate of sedimentation should be more favorable for formation of denser shell concentrations than sites of higher net rate of sedimentation (the low-dilution maxim of Kidwell 1991). Kidwell (1985, 1986a) built a theoretical framework for shell bed genesis and hypothesized that a model of shell bed formation could be cast mainly in terms of changes in sedimentation rate (this is known as the R-sediment model). As an alternative, Kidwell (1985, 1986a) proposed the R-hardpart model, which predicts that variations in dead-shell production and shell destruction rates primarily control the formation and preservation of shell beds. Thanks to the pioneering insights of these initial models, it is now clear that any satisfactory explanation of shell beds, and of taphonomic patterns in general, has to be rooted in sedimentation rate and hardpart-input rate. The R-sediment model has great power and robustness and is preferred because of its predictivity in terms of postmortem bias and biotic interactions (Kidwell 1986a). As many

 0094-8373/06/3202-0008/$1.00

shell beds are indeed preferentially associated with omission or erosional surfaces (Kidwell and Jablonski 1983; Kidwell 1989), the R-sediment model has been supported and successfully used in sequence stratigraphic and environmental analyses (Beckvar and Kidwell 1988; Kidwell 1993; Abbott 1997, 1998; Naish and Kamp 1997; Kondo et al. 1998; Fürsich and Pandey 2003; Yesares-García and Aguirre 2004; Cantalamessa et al. 2005; Parras and Casadío 2005). Sequence stratigraphic simulations also show that uniform stratigraphic distribution of fossils can be changed to nonrandom and clustered distribution because sequence architecture is strongly controlled by sedimentation rates (Holland 1995, 2000).

The R-sediment model (Kidwell 1985, 1986a) predicts that there will be positive correlation between shelliness and taphonomic alteration because shells are exposed longer when sediment dilution is low. Also, it predicts that with a decrease in sedimentation rate, an increase in shelliness will be associated with an increase in time-averaging (Fürsich and Aberhan 1990; Kowalewski et al. 1998), morphologic variation, and a change in community composition. However, the predictions of the R-hardpart model have not previously been explored fully.

Further analyses of the interplay between hardpart-input rate and sedimentation rate are necessary for better understanding of the dynamics of shell bed formation. First, it is of primary interest to know to what degree high shell density corresponds to original live abundance or whether it reflects only the effect of passive accumulation. In turn, it can be important to distinguish whether rarity of shells in shell-poor deposits is due to low hardpart-input rate or high background sedimentation rate. If the role of hardpart-input rates and sedimentation rates in formation of shell beds can be differentiated, these questions can be answered. Although community-level abundance in the fossil record is mostly assessed in terms of relative numerical abundance, the recognition of fossil macroinvertebrate populations with originally high density is also of ecologic importance because dense populations of shelly organisms play an important role as ecosystem engineers in aquatic habitats (Gutiérrez et al. 2003).

Second, in sections where variations in sedimentation rate are not obvious (e.g., because of lack of discontinuities), interpreting differences in shell beds exclusively in terms of changes in sedimentation limits the number of possible explanations for their origin.

Third, whereas the R-sediment model seems to work very well in some settings, dead-shell production and destruction rates appear to have played major roles in other settings. There are several examples of shell beds that probably reflect primarily a high rate of production of dead shells rather than lack of dilution alone. These can be related to productivity variations (Geary and Allmon 1990; Allmon 1993; Fürsich and Oschmann 1993; Allmon et al. 1995; Kowalewski et al. 2000; Nebelsick and Kroh 2002; Carroll et al. 2003) or catastrophic juvenile or adult mortality (Noe-Nygaard et al. 1987; Doyle and Macdonald 1993; Soja et al. 1996; Radley and Barker 1998). These three points are important in understanding the ecology of shell producers and destroyers on one hand, and the sedimentation regime on the other.

Recently, Tomašových et al. (2006) found a negative correlation between shelliness and alteration in Lower Jurassic brachiopod deposits of Morocco, a pattern that is not in agreement with predictions of the R-sediment model. To understand what might produce such a negative correlation in non-rapidly buried deposits, we developed a model in which hardpart-input and sedimentation rates could be varied. We used the model to derive predictions with respect to shelliness and assemblage-level alteration for four scenarios based on Kidwell's (1985, 1986a) approach (Fig. 1), and we then used the predictions of the model to interpret the Moroccan shell beds.

Modeling Autochthonous Shell Bed Formation

Shell bed formation can be ascribed to four major factors: (1) dead-shell production rate, (2) shell destruction rate, (3) sediment input rate, and (4) sediment output rate. The first two of these are equivalent to Kidwell's (1985,

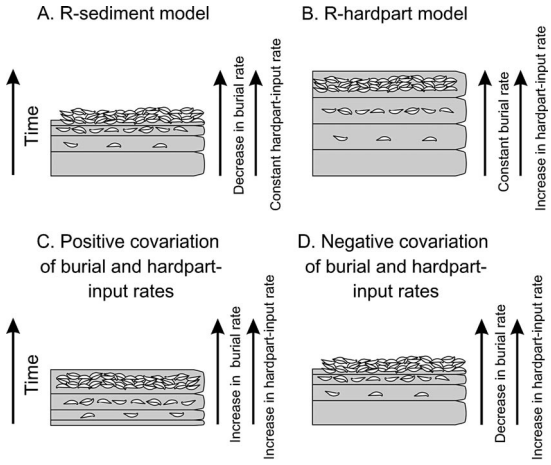

FIGURE 1. Four scenarios of increasing shelliness through time comparing differential hardpart-input rates with burial rates, based on Kidwell's (1985) approach. A, R-sediment model. B, R-hardpart model. C, Negative covariation of burial and hardpart-input rate. D, Positive covariation of burial and hardpart-input rate. For simplification, the thickness of beds is equivalent to net sedimentation rate. Note: Increase in burial rate/constant hardpart-input rate produces the opposite pattern to A. Constant burial rate/decrease in hardpart-input rate produces the opposite pattern to B. Decrease in burial rate/decrease in hardpart-input rate produces the opposite pattern to C. Increase in burial rate/decrease in hardpart-input rate produces the opposite pattern to D. Constant hardpart-input rate/constant burial rate produces no net trend in shelliness.

1986a) net rate of hardpart input, and the latter two to her net rate of sedimentation. The reason for dissecting the net rate of hard part input into two factors is that the two are driven by different causes and can be traced to or inferred from real biologic (e.g., population turnover) and taphonomic processes (e.g., environmental factors governing rate of destruction). The variation in sedimentation rate is modeled here as the variation in the length of exposure time, which is controlled by burial rate (i.e., we use the burial rate as a proxy for sedimentation rate). As this modeling is restricted to autochthonous shell beds, complex effects of reworking (Olszewski 2004) and transport (Miller and Cummins 1990, 1993) are not implemented here.

Two end-member hypotheses concerning the origin of shell beds phrased by Kidwell (1985, 1986a) can be considered: (1) the R-sediment model and 2) the R-hardpart model. In the R-sediment model, hardpart-input rates are kept constant while variation in sedimentation rates affects the degree of shell concentration. In this model, postmortem alteration correlates positively with shelliness. Although the R-sediment model is strictly applicable only to those shell beds with omission or erosional discontinuities (Kidwell 1985, 1986a), its predictions with respect to shelliness and postmortem bias are not sensitive to this constraint. In the R-hardpart model, sedimentation rates are kept constant while variation in hardpart-input rates influences the formation of shell concentrations. In this model, as will be shown, under varying shell destruction rates, a negative correlation between postmortem alteration and shelliness is expected.

Concept for Computation of Shelliness and Alteration in Shell Beds

In addition to a destruction half-life, which has been used in modeling studies (Powell 1992; Olszewski 1999), an alteration half-life is added to the model in order to compute assemblage-level alteration. The rate of shell destruction (λ_d) describes how rapidly shells are completely removed from a death assemblage. The rate of shell alteration (λ_a) describes how rapidly shells accrue postmortem damage in terms of fragmentation, bioerosion, dissolution, or other taphonomic variables. (Note that both of these variables are rate constants—i.e., they reflect proportional change rather than a fixed amount of change through time.) Naturally, alteration precedes final destruction in a taphonomic pathway (i.e., a destroyed shell is a shell that is so heavily altered that it cannot be detected in a death assemblage). It can therefore be assumed that under conditions of high rate of shell destruction, rate of shell alteration will also be high. Although both rates can be related to one causal factor, they are computed separately during modeling. They sum to a total λ, which is the total rate of loss of shells from their pristine state (their sum is not constrained to be less than one).

The modeling of shelliness and assemblage-level alteration in a shell bed is started by establishing an initial cohort with a certain number of shells in a death assemblage. When the shells in the death assemblage are exposed, they are destroyed and altered at constant proportional rates during consecutive

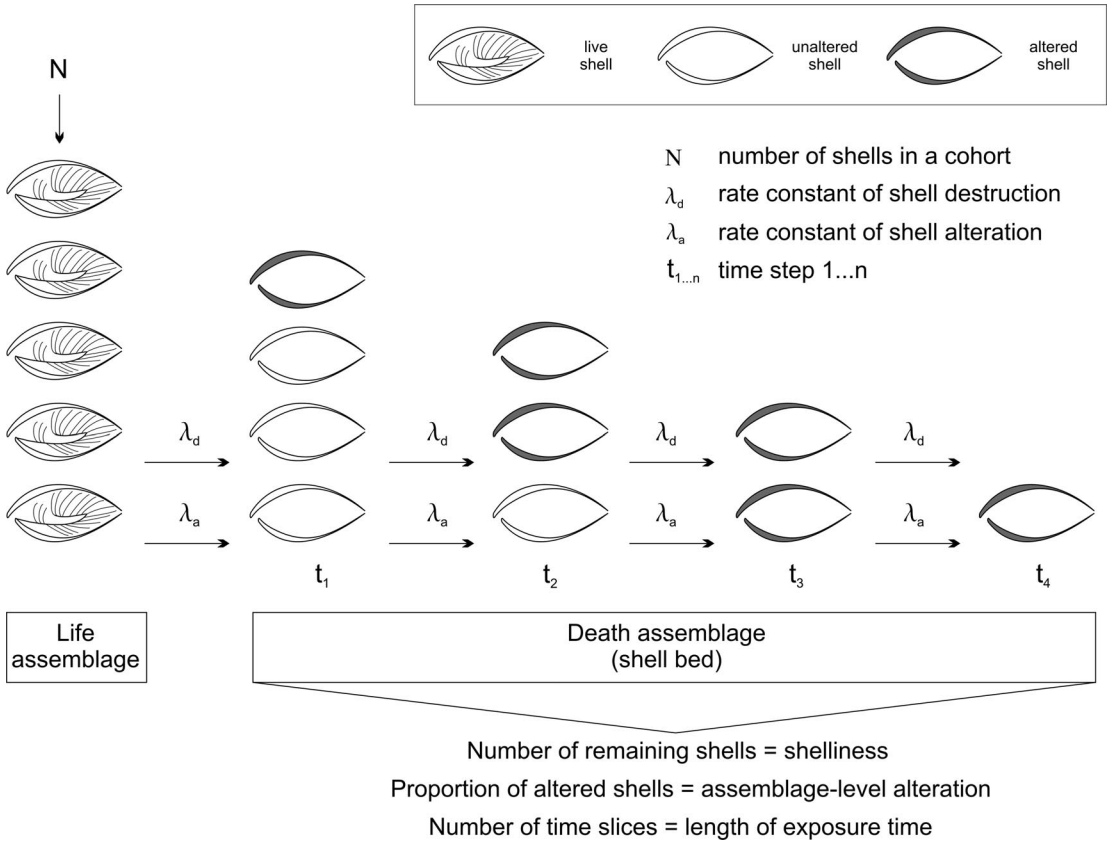

FIGURE 2. Cartoon of the modeling process. A cohort with a certain number of shells is added to a death assemblage. When the shells are exposed, they are destroyed and altered at constant rates during consecutive time steps. Therefore, the postmortem history of one cohort with a certain number of shells is tracked during its decay time. This distribution can also be understood as a snapshot of several cohorts that are successively added to the death assemblage. Combining all the cohorts in a shell bed, the total number of shells is a measure of shelliness and the total proportion of altered shells is a measure of assemblage-level alteration.

time steps (Fig. 2). The altered and unaltered shells are assumed to have an equal probability of destruction and alteration. The postmortem history of one cohort is thus tracked through its decay time. However, if this process is assumed to be ergodic, it can also be understood as a snapshot of several cohorts that were successively added to the death assemblage (Olszewski 2004). The total number of shells from all the cohorts in a shell bed is a measure of shelliness and the total proportion of altered shells is a measure of assemblage-level alteration (Fig. 2). The total proportion of altered shells is thus a function of the rate constant of destruction and the rate constant of alteration. As the destruction and alteration rates are active only when shells are exposed, the resulting age-frequency distribution of the cohorts with dead shells is here called the age-frequency distribution of exposed dead shells (EAFD). In other words, ages represent the duration of exposure, not necessarily the absolute age since time of death. If exposure time is modeled using an additional rate constant, then EAFD and postmortem age will be linearly related. The EAFD, with all parameters used in the computation of shelliness and assemblage-level alteration, is schematically shown in Figure 3.

1. Rate of Production of Dead Shells.—Rate of production of dead shells (i.e., population turnover) can be adjusted by varying the number of dead shells added into a death assemblage. One cohort may initially contain 10,100, or 1000 dead shells; the predicted result with regard to the proportion of surviving and al-

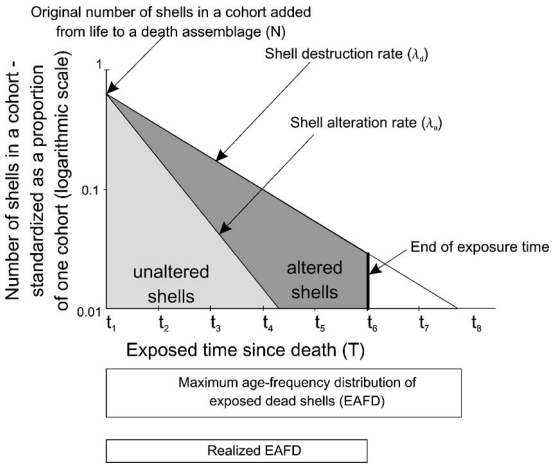

FIGURE 3. Scheme showing the terms used in the models and in computing the age-frequency distribution of exposed dead shells (EAFD). The y-axis with number of shells in a cohort is logarithmic. The entire shaded area represents all the shells in the death assemblage plotted against their ''exposed'' time since death. The light shaded area represents the number of shells that have not experienced any taphonomic alteration.

tered shells will be the same. Therefore, shelliness can be computed with an exponential equation as the sum of all shells that will survive beyond time t. If the proportion of a cohort falls below 0.01 in the tail of exponential distribution, the decay of a cohort is arbitrarily stopped. This case would correspond to a situation when the number of dead shells in a cohort with originally 100 shells is less than one. This means that the age-frequency distribution of exposed dead shells (EAFD) reaches its maximum attainable length at this point—further addition of time steps will produce no difference in the proportion of surviving and altered shells of a given age. Such an EAFD, in which the theoretically maximum possible length has been attained because the number of shells in a cohort has fallen below a certain minimum value, is termed *maximum* EAFD.

2. Rate of Shell Destruction (λ_d).—The simplest way to compute the number of surviving and destroyed dead shells is by assuming that for each time step during which shells are exposed, the probability of shell destruction is constant (Powell 1992; Flessa and Kowalewski 1994; Olszewski 1999, 2004). The number of surviving shells is computed with an exponential equation where the rate of destruction reflects the destruction half-life (Appendix 1). If destruction rate is high, most of dead shells that were added during one time step are destroyed during the next time step. If destruction rate is low, most of the shells are preserved. For the sake of simplicity, it is assumed that destruction is active only if a shell is exposed on the seafloor.

3. Rate of Shell Alteration (λ_a).—It is of interest to estimate what proportion of the surviving shells is represented by unaltered and by altered shells. The number of unaltered shells of a given age is computed with an exponential equation by summing the alteration half-life and the destruction half-life (Appendix 1). The number of altered shells can be computed as the difference between the number of surviving and unaltered dead shells. As was mentioned above, the assumption is that in high-destruction regimes, the rate of alteration will be higher than in low-destruction regimes. This assumption is supported by actualistic taphonomic studies (Powell et al. 1989; Callender et al. 1994, 2002).

4. Burial Rate.—The number of surviving and unaltered shells is calculated as the number of shells in a death assemblage exposed on the seafloor before burial. To transfer an exposed death assemblage into a buried death assemblage, we assume that during exposure each shell has an equal probability of being buried. The difference (in shelliness or postmortem assemblage-level alteration) between high and low rates of burial is thus defined by the difference in the length of exposure time. The end of exposure time can be understood as the time step at which the number of exposed shells in a cohort falls below some minimum value (i.e., most of the surviving shells will be buried). *Realized* EAFD is thus the EAFD that exists at the end of exposure time (controlled by the rate of burial, Fig. 3). If a cohort composed of a certain number of shells is ten time steps old, but it experienced exposure for only five time steps because of temporary burial and then exhumation, its apparent age with respect to surviving and altered shells is only five time steps.

Initial Conditions for Rates of Hardpart Input

With a hardpart-input rate as part of the theoretical concept, four initial end-member

TABLE 1. Initial conditions for hardpart-input rate regimes.

Long exposure time (66 time steps)	Rate of production of dead shells	Rate of destruction	Rate of alteration	Proportion of altered shells	Shelliness (number of shells, standardized as proportion of cohorts)
High production–low destruction	1 cohort/time step	0.069	0.069	51.2% altered shells	13.8 cohorts
Low production–low destruction	0.5 cohort/time step	0.069	0.069	51.2% altered shells	6.9 cohorts
High production–high destruction	1 cohort/time step	0.139	0.139	53.5% altered shells	6.7 cohorts
Low production–high destruction	0.5 cohort/time step	0.139	0.139	53.5% altered shells	3.4 cohorts
Short exposure time (10 time steps)	**Rate of production of dead shells**	**Rate of destruction**	**Rate of alteration**	**Proportion of altered shells**	**Shelliness (number of shells, standardized as proportion of cohorts)**
High production–low destruction	1 cohort/time step	0.069	0.069	27.6% altered shells	7 cohorts
Low production–low destruction	0.5 cohort/time step	0.069	0.069	27.6% altered shells	3.5 cohorts
High production–high destruction	1 cohort/time step	0.139	0.139	41.8% altered shells	5 cohorts
Low production–high destruction	0.5 cohort/time step	0.139	0.139	41.8% altered shells	2.5 cohorts

regimes are possible for a given burial rate. These are related to different rates of dead-shell production and shell destruction. They are designated here as a High production–Low destruction regime (HL), a High production–High destruction regime (HH), a Low production–Low destruction regime (LL), and a Low production–High destruction regime (LH). Shelliness and assemblage-level alteration are computed for each regime at given exposure time. For purpose of illustration and computation, arbitrarily set deterministic shell production and destruction rates (Table 1) are chosen in order to show variations in assemblage-level alteration and shelliness in the four main scenarios (Fig. 1). As will be shown below, the predictions for shelliness and alteration, which follow from the models, can be generalized beyond the values used for illustration.

One cohort per time step is used for the high production regime and 0.5 cohorts per time step for the low-production regime. The destruction half-life is ten time steps for the low-destruction regime. This means that after ten time steps, half of the dead shells that were initially added to a death assemblage will be destroyed. For the high-destruction regime, destruction half-life is five time steps. Similarly, the alteration half-life is five time steps for high-destruction regimes and ten time steps for low-destruction regimes. Production and destruction rates are thus set to vary by a factor of one, which means that net hardpart-input rate can vary by a factor of two. As follows from actualistic estimates of these rates (Davies et al. 1989), both can vary substantially, even by several orders of magnitude on short time scales. For example, carbonate production in shelf habitats ranges from several thousand grams of $CaCO_3$ m^{-2} $year^{-1}$ in oyster and coral reefs up to a few grams of $CaCO_3$ m^{-2} $year^{-1}$ in some siliciclastic habitats (Powell et al. 1989). Similarly, the range of variation in dissolution and bioerosion rates is markedly broad in modern shallow marine habitats (Sanders 2003). Therefore, the variations in rates used in the modeling are rather subtle when compared with real estimates.

As was summarized by Enos (1991), net sedimentation rates in marine environments vary by several orders of magnitude, and their estimation heavily depends on the time span of observation. Choosing appropriate burial rates for the models is thus difficult. The purpose here is to explore how shell beds might change when rate of burial changes from zero to some positive value. EAFD for high pro-

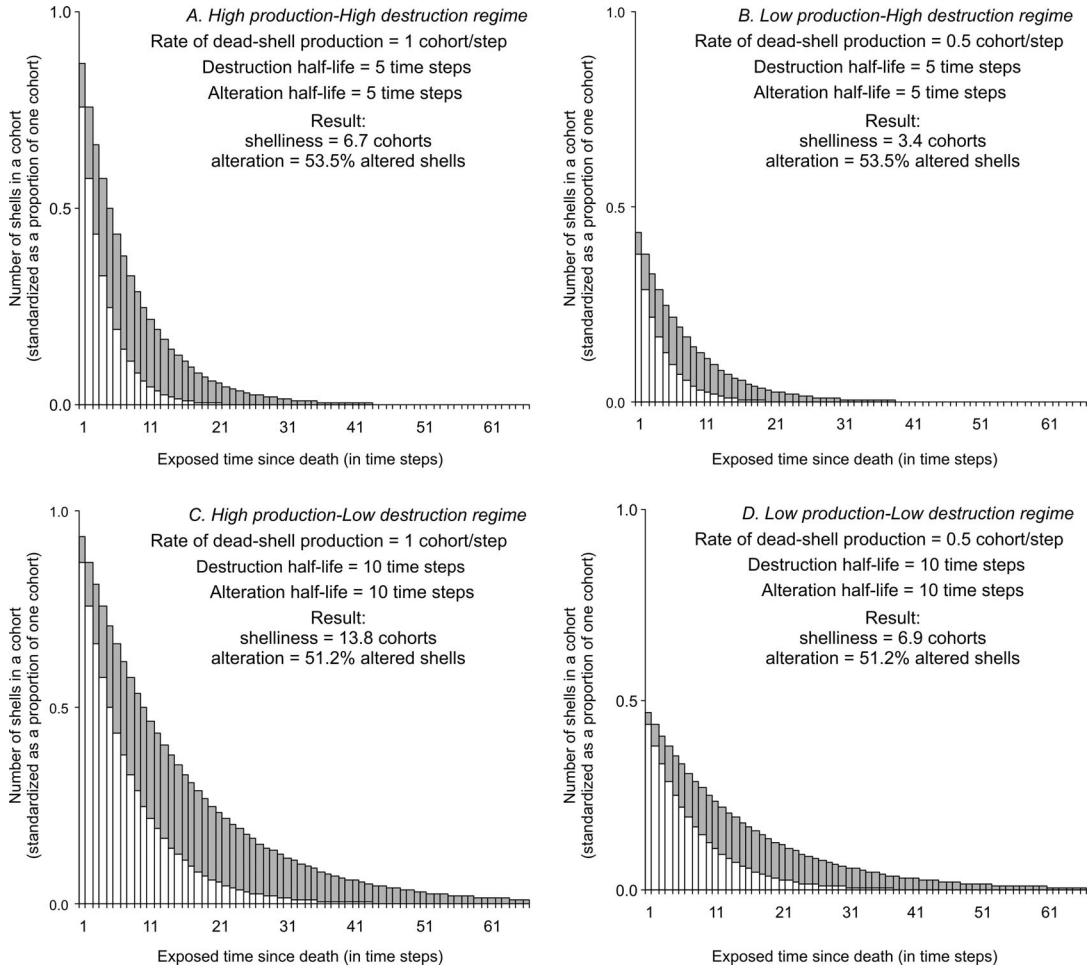

FIGURE 4. Computed age-frequency distributions of exposed dead shells (EAFD) with the proportions of altered and unaltered shells for four hardpart-input regimes. Parameter values were chosen to pinpoint the differences between them. A, High production–High destruction regime. B, Low production–High destruction regime. C, High production–Low destruction regime. D, Low production–Low destruction regime.

duction–low destruction regimes approaches its theoretical limit after 66 time steps because less than one shell is left at this point. Therefore, the length of exposure time with 66 time steps is used for situations when no shells are buried. In order to show the effect of burial, a ten-step exposure time is used (i.e., a cohort in the EAFD is buried after ten time steps). The EAFDs of four initial hardpart-input rate regimes for 66 time steps are shown in Figure 4. Computed shelliness and alteration for 66 time steps (maximum EAFDs) and ten time steps (realized EAFDs) are shown in Table 1.

Assumptions

1. Production Rates Are Continuous and Constant.—Maximum EAFD is attained when the number of shells falls under some minimum value. This means that there is an inherent limit for maximum shelliness and maximum proportion of altered shells. For example, in the HL regime with one cohort added per time step and a destruction half-life of ten time steps, the proportion of altered shells cannot exceed 51.2% (Table 1, Fig. 4). Although this may be counterintuitive, it is because of the assumption that rate of production of dead shells is continuous and constant at each time step. EAFD is thus always dominated by the cohorts that were produced in the last time step. In fact, natural populations fluctuate in density at various timescales. If production rates substantially decrease or even stop, this

can lead to the dominance of altered shells in long-dead cohorts (LDC). In contrast, at times of massive shell input, the EAFD will be dominated by recently dead cohorts (RDC) with low proportion of altered shells. In general, if input of dead shells substantially fluctuates through time, EAFD is unstable. In this case, the shelliness and assemblage-level alteration depend on the ratio of recently added cohorts and cohorts that have been dead for a long time. Fluctuating population density substantially affects the number of surviving juvenile shells in modern brachiopod death assemblages (Tomašových 2004). For the purpose of this study, it is assumed that rate of dead-shell production is constant.

2. Destruction Rates Follow an Exponential Function.—This is the simplest possibility for modeling destruction rates. However, there is some evidence that destruction rates have complex dynamics and may be nonlinear in time (Heinrich and Wefer 1986; Staff et al. 2002). For example, initially high dissolution rates observed in experimental conditions may decrease because of inversion of surface aragonite to more stable calcite (Morse et al. 1980). In contrast, the initial destruction rate may be lowered because of the protective effect of organic matrix and coatings (Glover and Kidwell 1993). Increase in destruction rates may then rapidly follow after degradation of organic materials. Also, some taphonomic agents can theoretically act against destruction, such as encrusters or precipitating crusts, making the shell more durable. Relaxing the two assumptions that dead-shell production and destruction rates are constants can make any simulation more realistic, however, it will produce further complexity.

Constant Hardpart-Input Rates and Varying Burial Rates

Results.—Constant hardpart input while burial rates vary is the end-member scenario equivalent to the R-sediment model (Kidwell 1985, 1986a). The basic pattern is that, if burial rate decreases (i.e., length of exposure time increases) and hardpart-input rates remain constant, both assemblage-level alteration and shelliness will increase (Fig. 5A; note that the diagrams are semi-logarithmic) and both will be *positively* correlated (Table 2). They correlate because any increase in exposure time increases the proportion of LDC with respect to RDC and also the total number of cohorts. Shells in RDC will show lower alteration than shells in LDC because of their shorter exposure time.

However, positive correlation occurs only in those cases when varying burial rates change the frequency distribution of RDC and LDC. Under constant burial rates, EAFD becomes stable when the number of shells in a cohort reaches a minimum in the tail of the exponential distribution. Therefore, with decreasing burial rates, neither shelliness nor alteration will increase beyond this boundary (Fig. 5B). For example, if EAFD is stable after 100 time steps, the increase of exposure time from 100 to 200 time steps will have no effect on shelliness and alteration. In the case when such maximum EAFDs are compared between regimes with different burial rates, no correlation between shelliness and alteration will result.

Discussion.—Kidwell's (1985) predictions with respect to shelliness and assemblage-level alteration are in accord with those derived from the models used here. If the maximum EAFD exceeds the length of exposure time delimited by burial rate, any change in the burial rate will change the frequency distribution of RDC and LDC. An increase in burial rate will produce better-preserved shells, because the proportion of recently dead shells with shorter exposure times will be higher. However, if decreasing burial rates exceed the length of maximum EAFD, no further increase in shelliness and alteration will result (Fig. 5B). This possibility, however, is based on the assumption that the rate of shell destruction follows exponential decay. If the rate of shell destruction substantially lowers or stops completely (i.e., because of diagenetic stabilization), shelliness and alteration may still increase with decreasing burial rates.

Varying Rates of Hardpart Input and Constant Burial Rates

Results.—Varying rates of hardpart input while burial rate is held constant is the end-member scenario equivalent to the R-hardpart

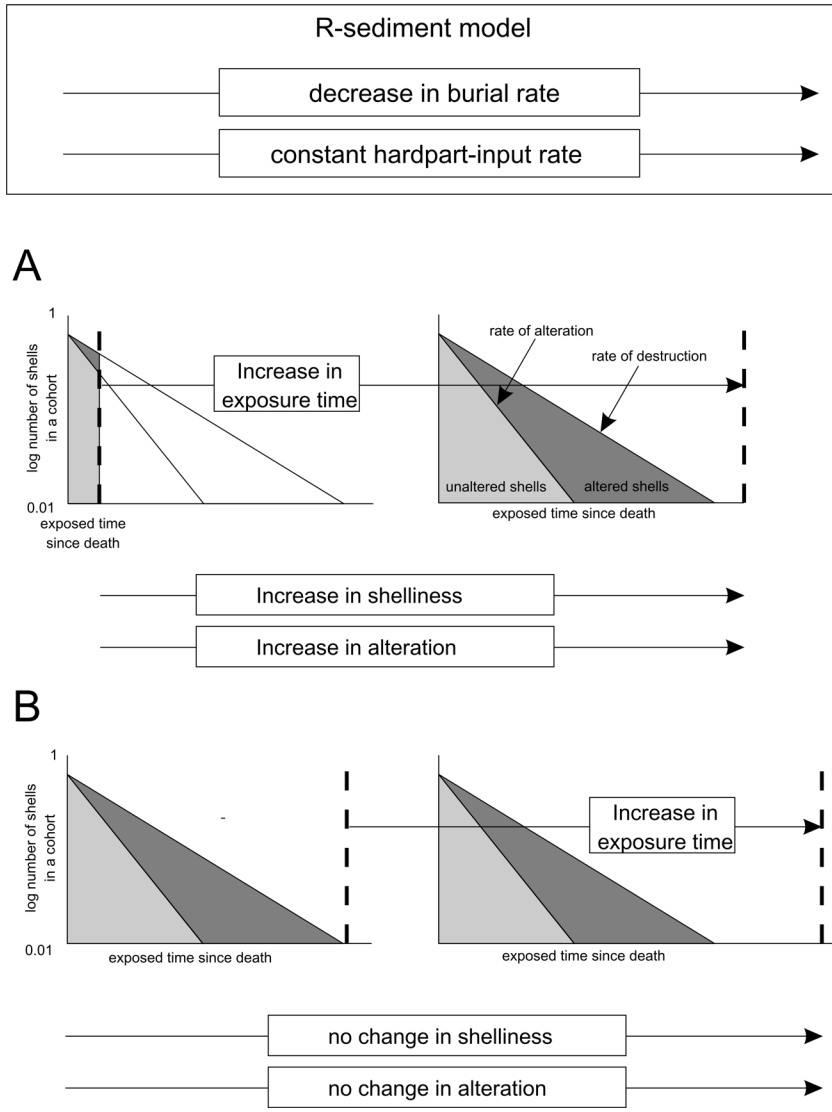

FIGURE 5. Predictions of a change in shelliness and alteration among regimes with constant rate of hardpart input but varying rate of burial. The y-axis with number of shells in a cohort is logarithmic. A, Increase in the length of exposure time leads to an increase in alteration and shelliness. This leads to a decrease in alteration and shelliness. B, Increase in length of exposure time does not affect EAFD.

model (Kidwell 1985, 1986a). Three causes can lead to an increase of the hardpart-input rate through time (Fig. 6). Either (1) rate of production of dead shells increases and rate of shell destruction remains constant (Fig. 6A), (2) rate of production of dead shells remains constant and rate of shell destruction decreases (Fig. 6B), or (3) rate of production of dead shells increases and rate of shell destruction decreases at the same time (Fig. 6C). Any increase in hardpart-input rate increases the length of maximum EAFD and thus the length of exposure time.

The first case leads to higher shelliness but the alteration levels do not change (Table 3, Fig. 6A). Therefore, there is no correlation between shelliness and alteration. In spite of EAFD being longer (it takes more time to destroy all shells because of higher input), the proportions of unaltered and altered shells remain the same. There are several possibilities that may change this prediction: Because the

TABLE 2. Comparison of predicted alteration and shelliness for constant hardpart-input rates and varying sedimentation rates.

Burial rate (exposure time)	Hardpart input regime	Assemblage-level alteration (proportion of altered shells)	Shelliness (standardized as a proportion of cohorts)	Alteration-shelliness correlation
Zero rate (66 time steps)	High production–low destruction	51.2%	13.8 cohorts	Positive
Positive rate (10 time steps)	High production–low destruction	27.6%	7 cohorts	
Zero rate (66 time steps)	Low production–low destruction	51.2%	6.9 cohorts	Positive
Positive rate (10 time steps)	Low production–low destruction	27.6%	3.5 cohorts	
Zero rate (66 time steps)	High production–high destruction	53.5%	6.7 cohorts	Positive
Positive rate (10 time steps)	High production–high destruction	41.8%	5 cohorts	
Zero rate (66 time steps)	Low production–high destruction	53.5%	3.4 cohorts	Positive
Positive rate (10 time steps)	Low production–high destruction	41.8%	2.5 cohorts	

length of maximum EAFD always increases with increasing hardpart-input rate, LDC in its tail may become buried because of positive burial rates and/or positive accretion of a shell bed, thus lowering the proportion of altered shells (Fig. 6D). This possibility will change the prediction with respect to the increase of rate of production of dead shells—although shelliness will still be higher, alteration will be lower. This leads to a *negative* correlation between shelliness and alteration, in contrast to the previous scenario with constant hardpart-input rates and varying burial rates.

In the second case (Fig. 6B), any decrease in destruction rates is associated with lower alteration (the proportion of unaltered shells increases) and higher shelliness (it takes more time to destroy shells because of lower destruction rates). Here, a *negative* correlation between shell alteration and shelliness is similarly expected. In the third case (Fig. 6C), the combined effect of higher dead-shell production rate and lower destruction rate leads similarly to a negative correlation between shelliness and alteration.

Discussion.—The scenarios with increased dead-shell production rate and/or decreased destruction rate show that variations in hardpart-input rates alone lead to predictable variations in postmortem bias (Table 4). This predictability arises because differential hardpart-input rates also govern exposure time and shape of EAFD. The prediction for varying hardpart-input rates is thus opposite to the R-sediment model—with increasing shelliness, postmortem bias (in terms of assemblage-level alteration) decreases. This major predicted difference with respect to the R-sediment model makes it possible to distinguish the effects of varying hardpart-input versus burial rates in shell bed genesis. Note that the higher the difference in hardpart-input rate, the higher the difference in shelliness and alteration. Therefore, varying hardpart-input rate by a factor of two, as in the models presented here, is a rather conservative estimate. With much higher production rate of dead shells and/or lower shell destruction rate, the difference in shelliness and alteration between regimes with low and high hardpart-input rate will be more pronounced.

Even when the shells in low-destruction regimes have longer exposure times because of longer maximum EAFD, their assemblage-level alteration is lower than in high-destruction regimes. An implicit assumption in most taphonomic analyses—that an increase in exposure times will lead to greater alteration—may not apply when regimes with different destruction rates are compared. It means that a shell bed with shorter exposure time but

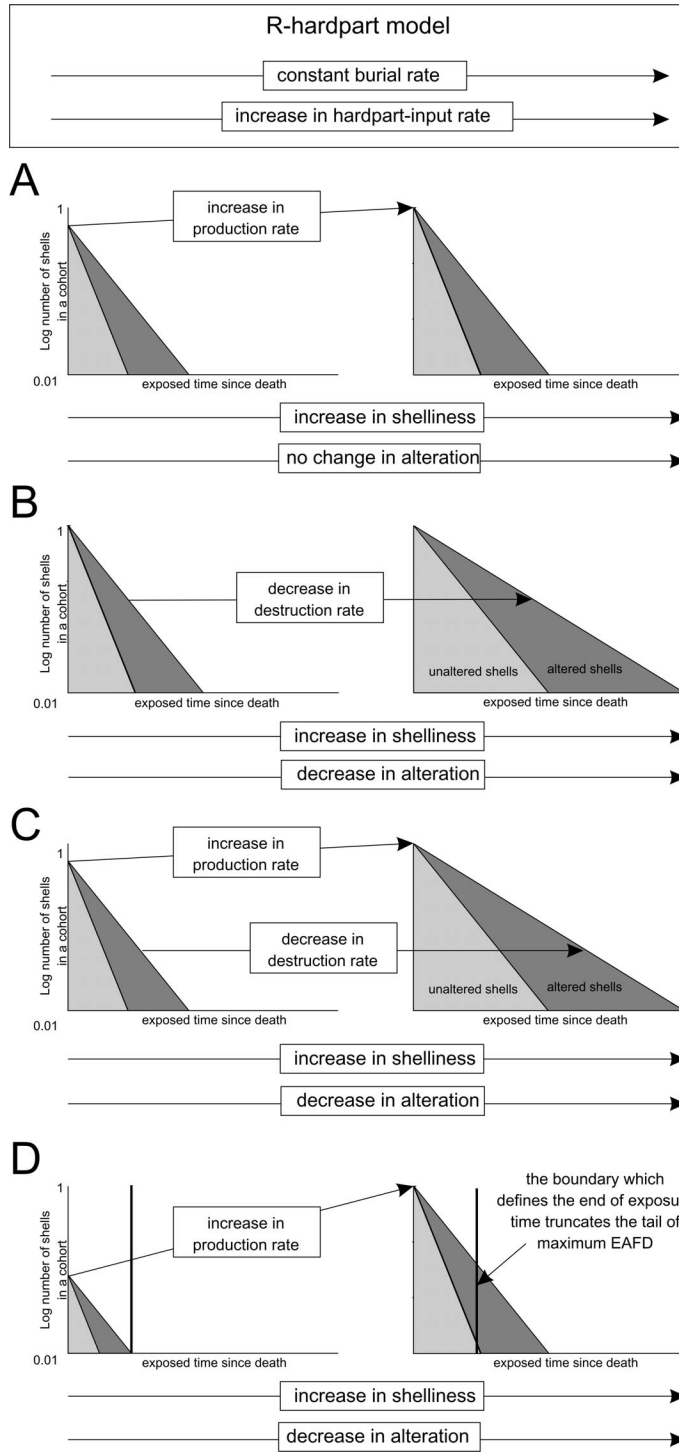

FIGURE 6. Predictions of a change in shelliness and alteration among regimes with varying hardpart-input rates but constant rate of burial. The y-axis (number of shells in cohort) is logarithmic. A, Increase in production rates leads to higher shelliness. B, Decrease in shell destruction rate leads to both higher shelliness and lower alteration. C, Increase in rate of production of dead shells combined with decrease in shell destruction rate leads to higher shelliness and lower alteration. D, Increase in hardpart-input rate (in this case rate of production of dead shells) leads to maximum EAFD, which may exceed the end of exposure time even under constant burial rate (e.g., because of positive accretion of shells, older shells are buried under younger shells). This also leads to higher shelliness and lower alteration.

TABLE 3. Comparison of predicted alteration and shelliness for varying hardpart-input rates and constant sedimentation rates.

Burial rate	Hardpart input regime	Assemblage-level alteration (proportion of altered shells)	Shelliness (standardized as a proportion of cohorts)	Damage-shelliness correlation
Zero	High production–low destruction	51.2%	13.8 cohorts	No correlation
Zero	Low production–low destruction	51.2%	6.9 cohorts	
Zero	High production–low destruction	51.2%	13.8 cohorts	Negative correlation
Zero	High production–high destruction	53.5%	6.7 cohorts	
Zero	High production–low destruction	51.2%	13.8 cohorts	Negative correlation
Zero	Low production–high destruction	53.5%	3.4 cohorts	
Zero	Low production–low destruction	51.2%	6.9 cohorts	Negative correlation
Zero	High production–high destruction	53.5%	6.7 cohorts	
Zero	Low production–low destruction	51.2%	6.9 cohorts	Negative correlation
Zero	Low production–high destruction	53.5%	3.4 cohorts	
Zero	High production–high destruction	53.5%	6.7 cohorts	No correlation
Zero	Low production–high destruction	53.5%	3.4 cohorts	

higher destruction rate will be more altered than a shell bed with longer exposure time and lower destruction rate. This effect of differential destruction rates may also indicate why the relationship between assemblage-level taphonomic preservation and time (comparable to the taphonomic clock concept based on individual shells) is not very strong (Flessa et al. 1993; Meldahl et al. 1997; Kidwell 1998).

Hardpart-Input Rates Covary with Burial Rates

Results.—In this scenario, increase in hardpart-input rate positively correlates with higher burial rate (Fig. 7). This can occur because (1) increase in rate of production of dead shells correlates with increased burial rates (Fig. 7A), (2) decrease in rate of shell destruction correlates with increased burial rates (Fig. 7B), or (3) increased burial rates correlate with both increased rate of production of dead shells and decreased rate of shell destruction (Fig. 7C). In each case, the increase in burial rates shortens the EAFD and increases the proportion of RDC. Invariably, this leads to lower assemblage-level alteration.

Higher rates of burial can result in lower shelliness (because realized EAFD is truncated by increased burial rate) but increase in hardpart-input rates can lead to higher shelliness (because maximum EAFD is longer). The resulting shelliness thus depends on the magnitude of increase in burial rate and the magnitude of increase in hardpart-input rate. For example, a massive increase in the rate of production of dead shells can lead to higher shelliness in spite of some increase in burial rates. A substantial increase in burial rates can lead to lower shelliness in spite of higher hardpart-input rate. Therefore, the resulting correlation between shelliness and alteration may be either positive or negative.

Discussion.—Because the prediction for correlation between shelliness and alteration in this scenario depends on the magnitude of change in burial and hardpart-input rates, sedimentologic or stratigraphic evidence is needed for evaluating whether there is a negative or positive covariation between burial and hardpart-input rates.

Hardpart-Input Rates Vary Inversely with Burial Rates

Results.—The reverse of the previous scenario is to assume that an increase in hardpart-input rate negatively covaries with increasing burial rate (Fig. 8). In this case, both decrease in burial rate (making the realized EAFD longer) and increase in hardpart-input rate invariably lead to higher shelliness.

Decrease in burial rates increases the proportion of LDC, but increase in dead-shell production rates increases the proportion of RDC. Therefore, when production rates of dead shells increase and burial rates decrease

TABLE 4. Summary of predictions for four scenarios based on approach of Kidwell (1985, 1986a).

	Shelliness	Assemblage-level alteration
Constant net hardpart-input rate (R-sediment model)		
Decrease in sedimentation rate	Increase	Increase
Constant sedimentation rate (R-hardpart model)		
Decrease in destruction rate	Increase	Decrease
Increase in production rate	Increase	No change/decrease
Decrease in destruction rate-increase in production rate	Increase	Decrease
Increase in net hardpart-input-increase in sedimentation		
Decrease in destruction rate	Increase/decrease	Decrease
Increase in production rate	Increase/decrease	Decrease
Decrease in destruction rate-increase in production rate	Increase/decrease	Decrease
Increase in net hardpart-input-decrease in sedimentation		
Decrease in destruction rate	Increase	Increase/decrease
Increase in production rate	Increase	Increase/decrease
Decrease in destruction rate-increase in production rate	Increase	Increase/decrease

(Fig. 8A), alteration can either increase or decrease. Lower destruction rates lead to lower proportion of altered shells, but decrease in burial rate can substantially lengthen EAFD, resulting in dominance of LDC with altered shells (Fig. 8B). As with increased dead-shell production rate, this case can lead to either higher or lower alteration. An increase in dead-shell production rate combined with a decrease in destruction rate can also lead to either a negative or positive correlation between shelliness and alteration (Fig. 8C).

Discussion.—As in the previous scenario, sedimentologic or stratigraphic evidence is needed to evaluate whether there is a negative or positive covariation between burial and hardpart-input rates. In any case, lower alteration in shell-rich beds relative to shell-poor beds points to a governing role by varying hardpart-input rates and cannot be explained by variations in burial rate alone. Inversely, positive correlation between shelliness and alteration cannot be explained solely by variations in hardpart-input rate.

Effects of Parameters on Shell Bed Formation

The modeling shows that all shell bed parameters (i.e., rate of shell destruction, rate of shell alteration, rate of dead-shell production, and rate of burial) may alone or in combination affect assemblage-level alteration and shelliness. Variations in shelliness and alteration are always associated with a change in the shape and length of the age-frequency distribution of exposed dead shells (Fig. 9). This distribution shows the distinct role of individual parameters with respect to their effect on shelliness and alteration.

Age-Frequency Distribution of Exposed Dead Shells.—The shape of EAFD of a death assemblage is determined by all of the principal shell bed parameters (Fig. 9). First, rate of production of dead shells determines the y-intercept of EAFD—the higher the input of dead shells, the more time it takes to destroy them. Second, under constant burial rate and constant production rate of dead shells, rate of shell destruction provides a limit for the maximum possible exposure time of dead shells (i.e., it determines the slope of EAFD). These two parameters define the maximum EAFD. Third, rate of burial may change the length of the EAFD. It means that exposure time of a death assemblage is not only a function of burial rates, but also of hardpart-input rates.

Shelliness.—Shelliness similarly reflects the effects of all three parameters. It increases with a higher rate of production of dead shells, a lower rate of shell destruction, or the combination of both. An increased burial rate may truncate the maximum EAFD and thus decrease shelliness.

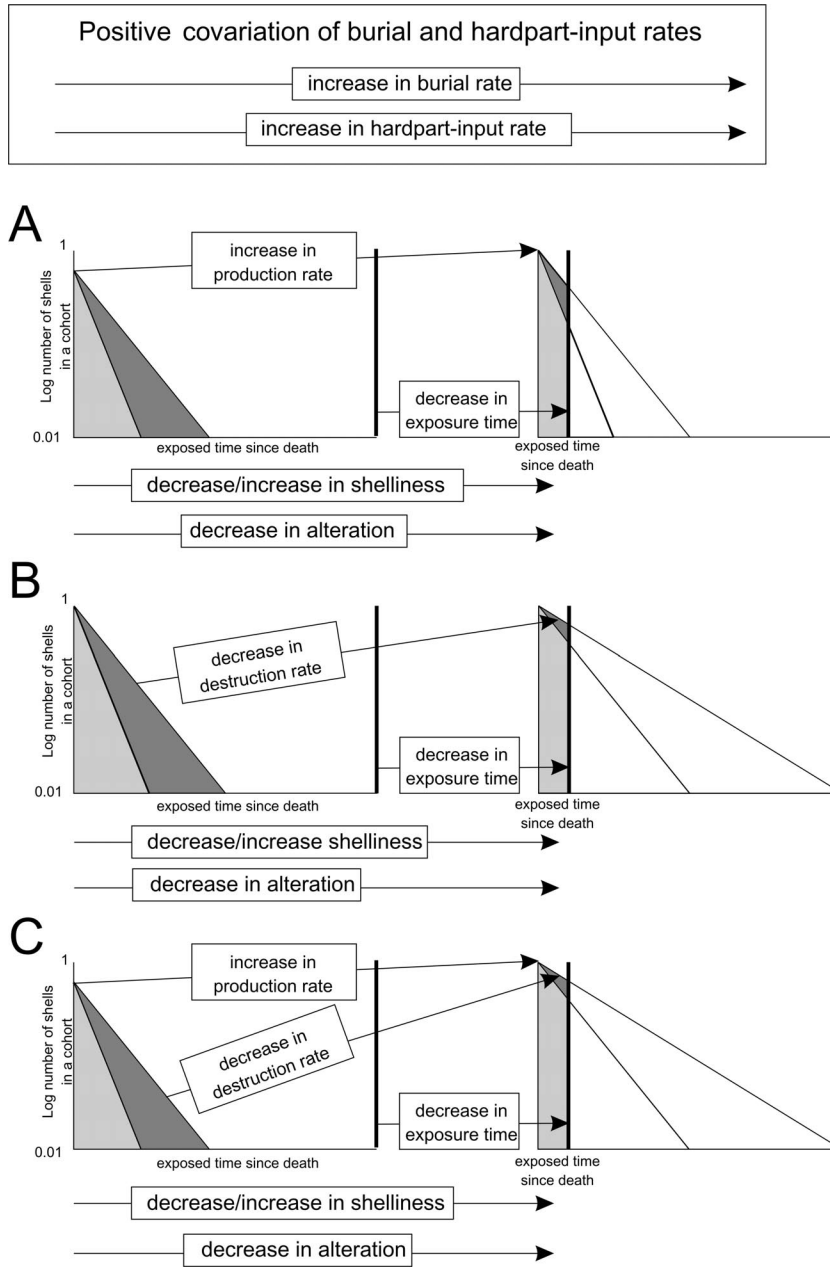

FIGURE 7. Predictions of a change in shelliness and alteration among regimes with positive covariation between increase in hardpart-input rate and increase in burial rate. All three cases lead to lower alteration. Shelliness may either increase or decrease. The y-axis (number of shells in cohort) is logarithmic. A, Increase in rate of production of dead shells is associated with increase in burial rate. B, Decrease in rate of shell destruction is associated with increase in burial rate. C, Increase in rate of production of dead shells combined with decrease in shell destruction rate is associated with increase in burial rate.

Assemblage-Level Alteration.—First, assemblage-level alteration depends on shell alteration rates, which are proportional to shell destruction rates (i.e., alteration decreases with lower destruction rates). Second, an increased burial rate may truncate the maximum EAFD, thus increasing the proportion of RDC (which will be less altered in contrast to LDC). As in

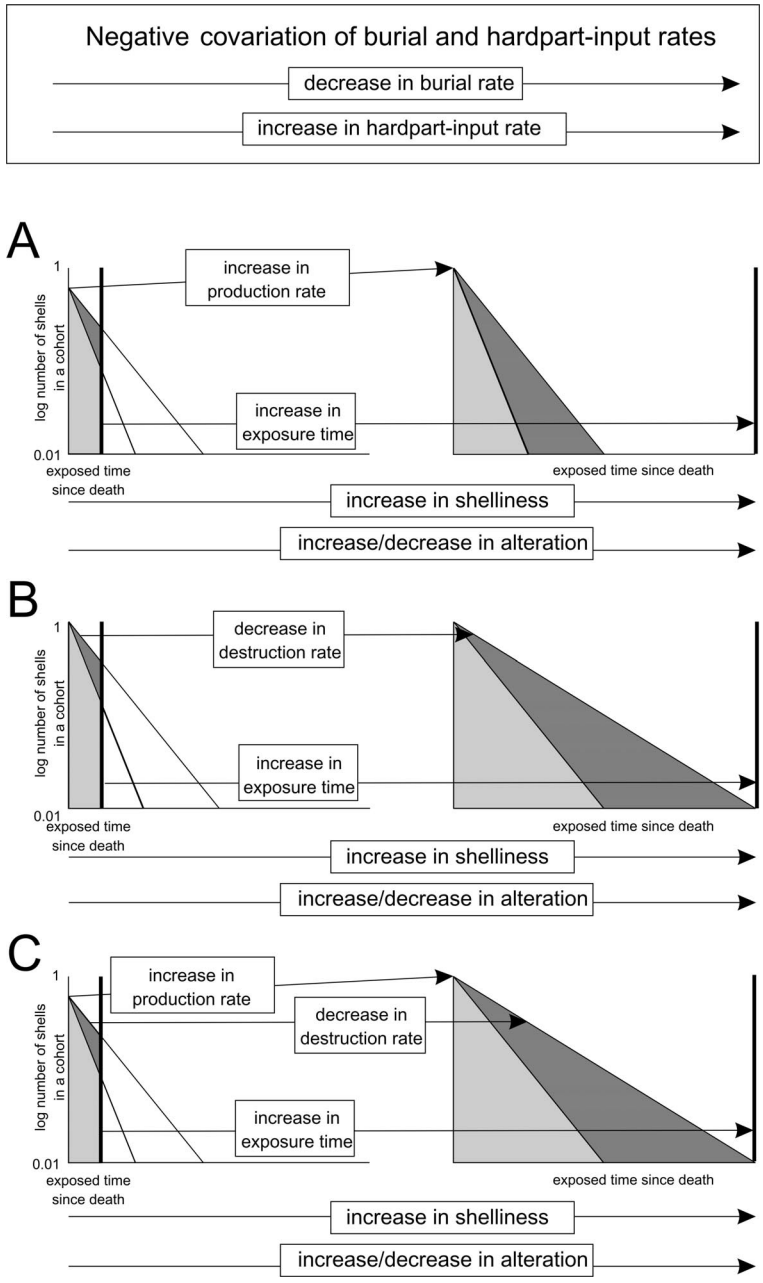

FIGURE 8. Predictions of change in shelliness and alteration among regimes with negative covariation between hardpart-input rate and burial rate. All three cases lead to higher shelliness. Alteration may either increase or decrease. The y-axis (number of shells in cohort) is logarithmic. A, Increase in rate of production of dead shells is associated with decrease in burial rate. B, Decrease in rate of shell destruction is associated with decrease in burial rate. C, Combined increase in rate of production of dead shells and decrease in shell destruction rate are associated with decrease in burial rate.

the case of the previous parameters, the rate of shell destruction, as well as burial rate, plays an important role. Third, a higher rate of dead shell production alone may increase the proportions of RDC and decrease postmortem alteration if the realized EAFD is truncated (e.g., owing to positive accretion of a shell bed or positive sediment input).

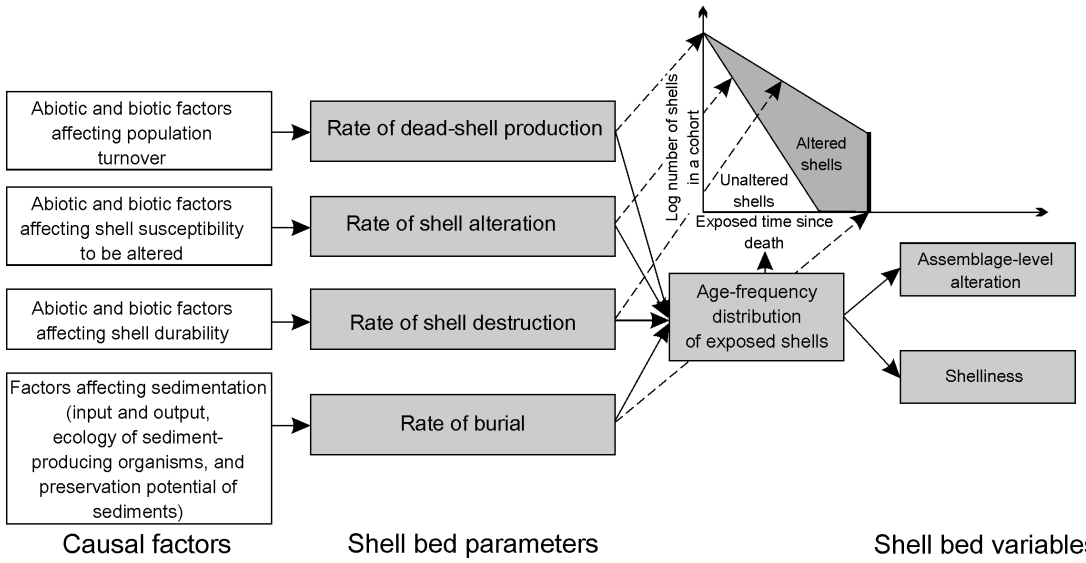

FIGURE 9. Theoretical concept showing the effects of shell bed parameters on the age-frequency distribution of exposed dead shells (EAFD). The EAFD determines shelliness and assemblage-level alteration.

Applying the Predictions to Data

Whether an increase in shelliness is in accord with the R-sediment or R-hardpart models is determined by comparing intensity of taphonomic alteration between shell-rich and shell-poor beds. Doing so requires a group of samples with varying shelliness from closely, vertically or horizontally, related deposits. Additional paleobiologic and sedimentologic evidence can be used for evaluating whether an observed correlation between shelliness and alteration in a given deposit indeed accurately predicts expected variations in burial and hardpart-input rates. The R-sediment model prediction of positive correlation between shelliness and alteration has been supported in several studies (e.g., Kidwell 1986b). To demonstrate that non-event deposits that show negative correlation between shelliness and alteration are indeed better explained by variations in hardpart-input rates, we compared alteration of shells between five shell-rich samples derived from a 1.5-m-thick, Lower Jurassic, densely packed shell bed in the Central High Atlas (Morocco) and ten shell-poor, loosely packed samples, which directly underlie or overlie this shell bed (Appendix 2). For this purpose, (1) the Spearman rank correlation between shelliness and assemblage-level alteration was calculated (Tomašových et al. 2006), and (2) to test whether shell-rich beds significantly differ in alteration from shell-poor beds, an analysis of similarities was performed (ANOSIM, Clarke and Green 1988). Both shell-poor and shell-rich samples are dominated mainly by the terebratulid brachiopod *Zeilleria rehmanni*. Brachiopod shelliness was estimated by the semiquantitative grain-solid method (Jaanusson 1972), and the assemblage-level alteration was estimated by evaluating proportions of six taphonomic variables counted on brachiopod specimens in thin-sections (Appendix 2). The proportion of shells in shell-poor, loosely packed samples is below 15%, and in shell-rich, densely packed samples, 15–25%. The Spearman coefficient is consistently negative for all variables and significant for disarticulation, fragmentation, and surface alteration (Table 5). ANOSIM shows that shell-rich samples significantly differ in their assemblage-level alteration from shell-poor samples ($R = 0.86$, $p = 0.0003$). In the pooled shell-rich samples, proportions of taphonomic variables are invariably lower than in the pooled shell-poor samples (Fig. 10). In terms of bootstrapped 95% confidence intervals, proportions of disarticulation, fragmentation, surface alteration, encrustation, and microbial crusts are significantly lower in shell-rich samples. The lower alteration in

TABLE 5. Summary of Spearman correlation coefficients comparing six taphonomic variables with shelliness. If the Bonferroni correction is applied, it lowers the alpha value to 0.0083 (0.05/6).

	Spearman *r*	*p*-value
Shelliness vs. disarticulation	−0.717	0.0026
Shelliness vs. fragmentation	−0.582	0.0228
Shelliness vs. alteration	−0.551	0.0330
Shelliness vs. bioerosion	−0.090	0.7247
Shelliness vs. microbial crusts	−0.478	0.0715
Shelliness vs. encrustation	−0.334	0.2234

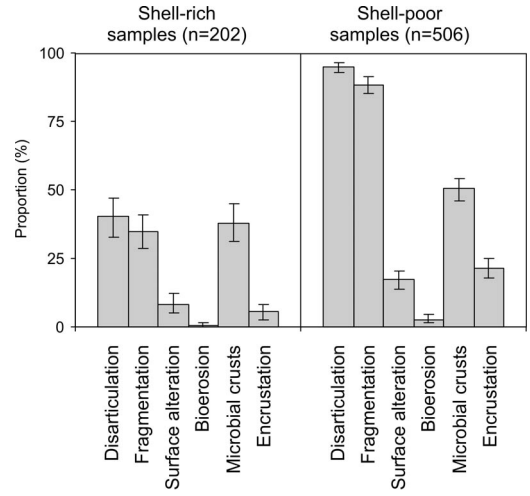

FIGURE 10. Comparison of assemblage-level alteration between pooled shell-rich and shell-poor samples. Five taphonomic variables show significantly lower proportions in shell-rich than in shell-poor samples (error bars show bootstrapped 95% confidence intervals). Based on data presented by Tomašových et al. (in press).

shell-rich samples from the Lower Jurassic carbonates indicates that variations in dead-shell production rate and shell destruction rate (i.e., R-hardpart model) governed their preservation style.

The role of increased hardpart-input rate in formation of the Lower Jurassic shell beds is supported by several arguments (Tomašových et al. 2006). First, community-level abundances of the main shell producer, *Z. rehmanni*, are higher in shell-rich than in shell-poor samples, indicating an increase in its production rate. Second, juveniles of *Z. rehmanni* are proportionally less common in shell-rich than in shell-poor samples, indicating a decrease in juvenile mortality rate and a higher production of adult shells. Third, sedimentologic evidence indicates that shell-rich samples are not associated with lower sedimentation rates than shell-poor samples (e.g., microbial crusts are thicker and more common in shell-poor samples), indicating that higher shelliness in shell-rich samples is not due to the lack of sediment. The lower alteration levels in shell-rich samples could reflect decreased shell destruction rates and/or shorter exposure time due to higher sediment input. The increase in shelliness in the Lower Jurassic deposits of Morocco thus primarily reflects an increase in population density of brachiopods, probably coupled with decreased shell destruction rates and/or shorter exposure times. When shell beds are interpreted to be driven by variations in hardpart-input rates, variations in shelliness can directly reflect fluctuations in population density of shell producers, and shell bed analyses can thus be useful in ecologic interpretations.

Conclusions

1. Our modeling approach complements other models because it allows computation of both shelliness and assemblage-level alteration. To estimate shelliness, we dissected hardpart-input rates into dead-shell production and shell destruction rates. To estimate assemblage-level alteration, we computed an alteration rate that describes how rapidly shells accrue postmortem damage. Modeling shell beds with varying hardpart-input rates (R-hardpart-model) provides the opposite prediction to the scenario of shell bed origin being driven by varying burial rates (R-sediment model). If burial rates are constant and hardpart-input rates vary, shelliness will increase with increased hardpart-input rate but assemblage-level alteration will decrease. This relationship leads to a negative correlation between shelliness and alteration, in contrast to a positive correlation predicted if varying burial rates govern shell bed formation. This difference in the predictions of the R-sediment and R-hardpart models makes it possible to distinguish whether a high shell density is driven primarily by high hardpart-input rate or by reduced burial rate leading to the lack of dilution. The Lower Jurassic brachiopod deposits of Morocco show a negative correlation be-

tween shelliness and alteration, giving support to the R-hardpart model. In this case, paleobiologic and sedimentologic data indicate that increased rate of production of dead shells and decreased rate of their destruction accounts for the origin of the Lower Jurassic shell-rich beds better than decreased burial rate. Assemblage-level alteration and shelliness are the data that are routinely collected by paleontologists and the correlation between them should thus be easily computable. Therefore, quantifying variations in alteration between shell-rich and shell-poor deposits can be used to infer whether high shell density is driven by changes in burial rates or hardpart-input rates.

2. We stress that postmortem alteration is a function not only of burial-driven exposure time, but also of varying hardpart-input rates. If an increase in hardpart-input rate covaries with increased burial rate, this invariably leads to lower alteration. If an increase in hardpart-input rate covaries with decreased burial rate, this always leads to higher shelliness. However, the predictions with respect to correlation between alteration and shelliness in both scenarios depend on the magnitude of change in burial rates and the magnitude of change in hardpart-input rates, and additional sedimentologic or stratigraphic evidence is necessary for evaluating these combined scenarios.

Acknowledgments

We thank Karl W. Flessa and Steven M. Holland for critical reviews, Tomasz K. Baumiller for editorial input and comments, M. Wilmsen for discussions, and M. Haddane for permissions that made the fieldwork in the Central High Atlas possible. This paper is supported by the Deutsche Forschungsgemeinschaft (Fu 131/26-1) and the Paleontological Society (S. J. Gould Award). This is Paleobiology Database publication number 36.

Literature Cited

Abbott, S. T. 1997. Mid-cycle condensed shellbeds from mid-Pleistocene cyclothems, New Zealand: implications for sequence architecture. Sedimentology 44:805–824.

———. 1998. Transgressive system tracts and onlap shellbeds from mid-Pleistocene sequences, Wanganui Basin, New Zealand. Journal of Sedimentary Research 68:253–268.

Allmon, W. D. 1993. Age, environment and mode of deposition of the densely fossiliferous Pinecrest Sand (Pliocene of Florida): implications for the role of biological productivity in shell bed formation. Palaios 8:183–201.

Allmon, W. D., M. P. Spizuco, and D. S. Jones. 1995. Taphonomy and paleoenvironment of two turritellid-gastropod-rich beds, Pliocene of Florida. Lethaia 28:75–83.

Beckvar, N., and S. M. Kidwell. 1988. Hiatal shell concentrations, sequence analysis, and sealevel history of a Pleistocene coastal alluvial fan, Punta Chueca, Sonora. Lethaia 21:257–270.

Callender, W. R., E. N. Powell, and G. M. Staff. 1994. Taphonomic rates of molluscan shells placed in autochthonous assemblages on the Louisiana continental slope. Palaios 9:60–73.

Callender, W. R., G. M. Staff, and K. M. Parsons-Hubbard, et al. 2002. Taphonomic trends along a forereef slope: Lee Stocking Island, Bahamas. I. Location and water depth. Palaios 17:50–65.

Cantalamessa, G., C. Di Celma, and L. Ragaini. 2005. Sequence stratigraphy of the Punta Ballena Member of the Jama Formation (Early Pleistocene, Ecuador): insights from integrated sedimentologic, taphonomic and paleoecologic analysis of molluscan shell concentrations. Palaeogeography, Palaeoclimatology, Palaeoecology 216:1–25.

Carroll, M., M. Kowalewski, M. G. Simões, and G. A. Goodfriend. 2003. Quantitative estimates of time-averaging in terebratulid brachiopod shell accumulations from a modern tropical shelf. Paleobiology 29:381–402.

Clarke, K. R., and R. H. Green. 1988. Statistical design and analysis for a ''biological effects'' study. Marine Ecology Progress Series 46:213–226.

Davies, D. J., E. N. Powell, and R. J. Stanton, Jr. 1989. Relative rates of shell dissolution and net sediment accumulation—a commentary: can shell beds form by the gradual accumulation of biogenic debris on the sea floor? Lethaia 22:207–212.

Doyle, P., and D. I. M. Macdonald. 1993. Belemnite battlefields. Lethaia 26:65–80.

Enos, P. 1991. Sedimentary parameters for computer modeling. Kansas Geological Survey Bulletin 233:62–99.

Flessa, K. M., and M. Kowalewski. 1994. Shell survival and time-averaging in nearshore and shelf environments: estimates from the radiocarbon literature. Lethaia 27:153–165.

Flessa, K. M., A. H. Cutler, and K. H. Meldahl. 1993. Time and taphonomy: quantitative estimates of time-averaging and stratigraphic disorder in a shallow marine habitat. Paleobiology 19:266–286.

Fürsich, F. T., and M. Aberhan. 1990. Significance of time-averaging to palaeocommunity analysis. Lethaia 23:143–152.

Fürsich, F. T., and W. Oschmann. 1993. Shell beds as tools in basin analysis: the Jurassic of Kachchh, western India. Journal of Geological Society, London 150:169–185.

Fürsich, F. T., and D. K. Pandey. 2003. Sequence stratigraphic significance of sedimentary cycles and shell concentrations in the Upper Jurassic-Lower Cretaceous of Kachchh, western India. Palaeogeography, Palaeoclimatology, Palaeoecology 193: 285–309.

Geary, D. H., and W. D. Allmon. 1990. Biological and physical contributions to the accumulation of strombid gastropods in a Pliocene shell bed. Palaios 5:259–272.

Glover, C. P., and S. M. Kidwell. 1993. Influence of organic matrix on the post-mortem destruction of molluscan shells. Journal of Geology 101:729–747.

Gutiérrez, J., C. G. Jones, D. L. Strayer, and O. O. Iribarne. 2003. Mollusks as ecosystem engineers: the role of shell production in aquatic habitats. Oikos 101:79–90.

Heinrich, R., and G. Wefer. 1986. Dissolution of biogenic car-

bonates: effects of skeletal structure. Marine Geology 71:341–362.
Holland, S. M. 1995. The stratigraphic distribution of fossils. Paleobiology 21:92–109.
———. 2000. The quality of the fossil record: a sequence stratigraphic perspective. *In* D. H. Erwin and S. L. Wing, eds. Deep time. Paleobiology 26(Suppl. to No. 4):103–147.
Jaanusson, V. 1972. Constituent analysis of an Ordovician limestone from Sweden. Lethaia 5:217–237.
Kidwell, S. M. 1985. Palaeobiological and sedimentological implications of fossil concentrations. Nature 318:457–460.
———. 1986a. Models for fossil concentrations: paleobiologic implications. Paleobiology 12:6–24.
———. 1986b. Taphonomic feedback in Miocene assemblages: testing the role of dead hardparts in benthic communities. Palaios 1:239–255.
———. 1989. Stratigraphic condensation of marine transgressive records: origin of major shell deposits in the Miocene of Maryland. Journal of Geology 97:1–24.
———. 1991. The stratigraphy of shell concentrations. *In* P. A. Allison and D. E. G. Briggs, eds. Taphonomy: releasing the data locked in the fossil record. Topics in Geobiology 9:115–129. Plenum, New York.
———. 1993. Taphonomic expressions of sedimentary hiatuses: field observations on bioclastic concentrations and sequence anatomy in low, moderate and high subsidence settings. Geologische Rundschau 82:189–202.
———. 1998. Time-averaging in the marine fossil record: overview of strategies and uncertainties. Geobios 30:977–995.
Kidwell, S. M., and D. Jablonski. 1983. Taphonomic feedback: ecological consequences of shell accumulations. *In* M. J. S. Tevesz and P. L. McCall, eds. Biotic interactions in recent and fossil benthic communities. Topics in Geobiology 3:195–248. Plenum, New York.
Kondo, Y., S. T. Abbott, and A. Kitamura, et al. 1998. The relationship between shellbed type and sequence architecture: examples from Japan and New Zealand. Sedimentary Geology 122:109–127.
Kowalewski M., G. A. Goodfriend, and K. W. Flessa. 1998. High-resolution estimates of temporal mixing within shell beds: the evils and virtues of time-averaging. Paleobiology 24:287–304.
Kowalewski, M., G. E. A. Serrano, K. W. Flessa, and G. A. Goodfriend. 2000. Dead delta's former productivity: two trillion shells at the mouth of the Colorado river. Geology 28:1059–1062.
Meldahl, K. E., K. W. Flessa, and A. H. Cutler. 1997. Time-averaging and postmortem skeletal survival in benthic fossil assemblages: quantitative comparisons among Holocene environments. Paleobiology 23:207–229.
Miller, A. I., and H. Cummins. 1990. A numerical model for the formation of fossil assemblages: estimating the amount of post-mortem transport along environmental gradients. Palaios 5:303–316.
———. 1993. Using numerical models to evaluate the consequences of time-averaging in marine fossil assemblages. *In* S. M. Kidwell and A. K. Behrensmeyer, eds. Taphonomic approaches to time resolution in fossil assemblages. Short Courses in Paleontology 6:151–168. Paleontological Society, Knoxville, Tenn.
Morse, J. W., A. Mucci, and F. J. Millero. 1980. The solubility of calcite and aragonite in seawater of 35‰ salinity at 25°C and atmospheric pressure. Geochimica et Cosmochimica Acta 44: 85–94.
Naish, T., and P. J. J. Kamp. 1997. Sequence stratigraphy of sixth-order (41 k.y.) Pliocene-Pleistocene cyclothems, Wanganui Basin, New Zealand: a case for the regressive systems tract. Geological Society of America Bulletin 109:978–999.
Nebelsick, J. H., and A. Kroh. 2002. The stormy path from life to death assemblages: the formation and preservation of mass accumulations of fossil sand dollars. Palaios 17:378–393.
Noe-Nygaard, N., F. Surlyk, and S. Piasecki. 1987. Bivalve mass mortality caused by toxic dinoflagellate blooms in a Berriasian-Valanginian lagoon, Bornholm, Denmark. Palaios 2:263–273.
Olszewski, T. D. 1999. Taking advantage of time-averaging. Paleobiology 25:226–238.
———. 2004. Modeling the influence of taphonomic destruction, reworking, and burial on time-averaging in fossil accumulations. Palaios 19:39–50.
Parras, A., and S. Casadío. 2005. Taphonomy and sequence stratigraphic significance of oyster-dominated concentrations from the San Julián Formation, Oligocene of Patagonia, Argentina. Palaeogeography, Palaeoclimatology, Palaeoecology 217:47–66.
Powell, E. N. 1992. A model for death assemblage: can sediment shelliness be explained? Journal of Marine Research 50:229–265.
Powell, E. N., G. M. Staff, D. J. Davies, and W. R. Callender. 1989. Macrobenthic death assemblages in modern marine environments: formation, interpretation, and application. Reviews in Aquatic Sciences 1:555–589.
Radley, J. D., and M. J. Barker. 1998. Palaeoenvironmental analysis of shell beds in the Wealden Group (Lower Cretaceous) of the Isle of Wight, southern England: an initial account. Cretaceous Research 19:489–504.
Sanders, D. 2003. Syndepositional dissolution of calcium carbonate in neritic carbonate environments: geological recognition, processes, potential significance. Journal of African Earth Sciences 36:99–134.
Schäfer, K. 1969. Vergleichs-Schaubilder zur Bestimmung des Allochemgehalts bioklastischer Karbonatgesteine. Neues Jahrbuch für Geologie und Paläontologie, Monatshefte 1969: 173–184.
Soja, C. M., K. E. Gobetz, and J. Thibeau, et al. 1996. Taphonomy and paleobiological implications of Middle Devonian (Eifelian) nautiloid concentrates, Alaska. Palaios 11:422–436.
Staff, G. M., R. W. Callender, and E. N. Powell, et al. 2002. Taphonomic trends along a forereef slope: Lee Stocking Island, Bahamas. II. Time. Palaios 17:66–83.
Tomašových, A. 2004. Postmortem durability and population dynamics affecting the fidelity of brachiopod size-frequency distributions. Palaios 19:477–496.
Tomašových, A., F. T. Fürsich, and M. Wilmsen. 2006. Preservation of autochthonous shell beds by positive feedback between increased hardpart-input rates and increased sedimentation rates. Journal of Geology (in press).
Yesares-García, J., and J. Aguirre. 2004. Quantitative taphonomic analysis and taphofacies in lower Pliocene temperate carbonate-siliciclastic mixed platform deposits (Almería-Níjar basin, SE Spain). Palaeogeography, Palaeoclimatology, Palaeoecology 207:83–103.

Appendix 1

Using the assumptions of the model presented in the text, we can calculate explicitly the proportion of altered shells expected in a shell bed. Once a shell has entered the death assemblage, it has a constant probability of being destroyed in any time interval, so in every time interval the total number of shells decreases by a constant proportion (λ_d = rate constant of shell destruction). Change in the number of shells through time is described by the following equation:

$$\frac{dN}{dt} = -\lambda_d N, \tag{1}$$

where N = proportion of shells remaining from original cohort and t = time.

When integrated, equation (1) yields the exponential function for the proportion of original shells surviving to time t:

$$N(t) = e^{-\lambda_d t} \tag{2}$$

Integrating $N(t)$ over time gives the expected number of shells in a death assemblage, assuming that each additional cohort is identical to all the others in size and rate of loss (Fig. A1):

$$\int_0^\infty N(t)\,dt = \int_0^\infty e^{-\lambda_d t}\,dt = -\frac{1}{\lambda_d} e^{-\lambda_d t}\Big|_0^\infty = \frac{1}{\lambda_d}. \tag{3}$$

What proportion of these surviving shells is expected to be taphonomically altered? Just as the proportion of shells destroyed in each time interval is assumed to be constant, the proportion that is taphonomically modified can also be assumed to be constant (λ_a = rate constant of shell alteration). The chance of a shell surviving to a certain age and not being altered is governed by the sum of λ_a and λ_d, both of which are proportions per unit time:

$$\frac{dN_s}{dt} = -(\lambda_a + \lambda_d)N, \tag{4}$$

where N_s = proportion of shells surviving unaltered.

Using analogous reasoning as above, the expected number of surviving, unaltered shells in the death assemblage is

$$\int_0^\infty e^{-(\lambda_a+\lambda_d)t}\,dt = -\frac{1}{\lambda_a + \lambda_d} e^{-(\lambda_a+\lambda_d)t}\Big|_0^\infty = \frac{1}{\lambda_a + \lambda_d}. \tag{5}$$

The expected number of altered shells in the shell bed is therefore

$$\frac{1}{\lambda_d} - \frac{1}{\lambda_a + \lambda_d}, \tag{6}$$

and the proportion of altered shells in the shell bed itself is

$$P_\infty = \frac{\dfrac{1}{\lambda_d} - \dfrac{1}{\lambda_a + \lambda_d}}{\dfrac{1}{\lambda_d}} = \frac{\lambda_a}{\lambda_a + \lambda_d}. \tag{7}$$

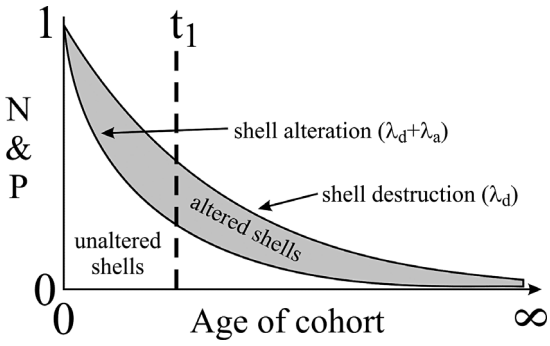

FIGURE A1. Age distribution of shells (N, upper curve) and proportion of unaltered shells (P, lower curve). Upper curve is controlled by rate constant of shell destruction (λ_d). Lower curve is controlled by the sum of λ_d and λ_a, the rate constant of postmortem shell alteration. Shaded region indicates the proportion of taphonomically altered shells.

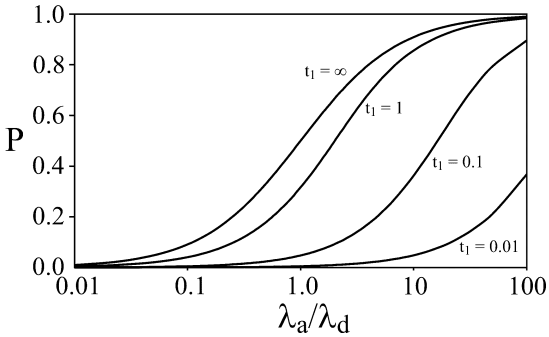

FIGURE A2. Influence of burial on the proportion of taphonomically altered shells in a shell bed (P). Truncation time of burial (t_1) has been non-dimensionalized by multiplying it by $1/\lambda_d$. For the theoretically untruncated distribution ($t_1 = \infty$), 0.5 of all shells in the accumulation are taphonomically altered when $\lambda_a = \lambda_d$. When λ_a is $<0.1\lambda_d$ or $>10\lambda_d$, most shells are either unaltered or altered, respectively. When shell bed accumulation is truncated before shells can develop the long exponential tail seen in Figure A1, a greater rate of alteration is required for a measurable proportion of shells to show taphonomic modification.

Equations (1) through (7) all assume an exposed time-since-death long enough for the shell age distribution to approach its theoretical limit. Truncating the duration of shell bed accumulation changes both the proportion of surviving shells of the original cohort and the proportion of altered shells in the shell bed. To take this factor into account in the mathematical description requires integrating equation (2) from the starting time ($t = 0$) to the time when burial ends the input of additional cohorts of dead shells (t_1):

$$\int_0^{t_1} N(t)\,dt = \int_0^{t_1} e^{-\lambda_d t}\,dt = -\frac{1}{\lambda_d} e^{-\lambda_d t}\Big|_0^{t_1} = \frac{1}{\lambda_d}(1 - e^{-\lambda_d t_1}). \tag{8}$$

In this case, the total number of unaltered shells in the shell bed is

$$\int_0^{t_1} e^{-(\lambda_a+\lambda_d)t}\,dt = -\frac{1}{\lambda_a + \lambda_d} e^{-(\lambda_a+\lambda_d)t}\Big|_0^{t_1}$$

$$= \frac{1}{\lambda_a + \lambda_d}[1 - e^{-(\lambda_a+\lambda_d)t_1}], \tag{9}$$

and the total number of altered shells in the shell bed is therefore

$$\frac{1}{\lambda_d}(1 - e^{-\lambda_d t_1}) - \frac{1}{\lambda_a + \lambda_d}[1 - e^{-(\lambda_a+\lambda_d)t_1}]. \tag{10}$$

The expected proportion of altered shells in a shell bed buried before it begins to approximate the theoretical distribution expected in an infinite amount of time is (Fig. A2):

$$P_{t_1} = 1 - \frac{\lambda_d}{\lambda_a + \lambda_d} \frac{1 - e^{-(\lambda_a+\lambda_d)t_1}}{1 - e^{-\lambda_a t_1}} \tag{11}$$

Appendix 2

Details about the stratigraphic section, sampling and data analyses are given in Tomašových et al. (2006). Shelliness was estimated by a visual semi-quantitative comparative method as the proportion of bioclasts in a thin-section (Schäfer 1969). The grain-bulk method could lead to artificial differences in shelliness if samples with differential proportions of articulated shells were compared. Due to this inflation, the grain-solid method (i.e., area of solid skeletal material is estimated only) is used in this study (Jaanusson 1972). The proportions of disarticulation, fragmentation, encrustation, surface alteration, bioe-

rosion, and microbial crusts were scored for brachiopods larger than 1 mm in thin-sections. Fragmentation refers to any breakage visible in a thin-section. Encrustation refers to foraminifers, bryozoans, serpulids, agglutinated polychaetes, sponges and oysters. Surface alteration denotes any microscopic irregularities, pitting or delamination on the interior or exterior surfaces of brachiopod valves (i.e., it can be related to abrasion, maceration, dissolution or very fine microbioerosion). Bioerosion refers to borings larger than 10 μm in diameter. Microbial crusts refer to dark, non-destructive, micritic or peloidal coatings. With the exception of disarticulation and fragmentation, only those specimens which showed taphonomic alteration on both sides of the valves were scored. Analysis of similarities (ANOSIM) tests whether average rank distance within shell-rich or shell-poor samples, based on Manhattan distance, is significantly lower than average rank distance between shell-rich and shell-poor samples (Clarke and Green 1988). The test statistic (R) attains values from −1 to 1. It is approximately zero if the null hypothesis is true. Large values close to one are indicative of complete difference in assemblage-level alteration. Significance levels are computed with a general randomization Monte Carlo approach. The confidence intervals were derived from the bootstrapped mean-frequency distribution (resampled with replacements, with number of replacements corresponding to the number of specimens in the shell-rich and shell-poor samples, and iterated 1000 times).